NOTES AND CORRESPONDENCE

On Airflow Boundary Layer above the Profile of Long Waves

SHI-CAI SUN[1] AND JIN WU

Air-Sea Interaction Laboratory, College of Marine Studies, University of Delaware, Lewes, DE 19958

4 January 1984 and 11 June 1984

ABSTRACT

Experiments were performed on the airflow boundary layer over pre-existing long waves. The latter were verified to have smoothening effects on the wind-disturbed water surface. The wind stress was found to be modulated, with a larger stress on the windward face of long waves.

1. Introduction

Many studies have been conducted on the structure of airflow boundary layer over a water surface. Most results were longitudinally averaged over the profile of dominant waves to provide a gross representation of the wind–wave interacting process over a large area of the sea surface. There are, however, evidences that actual physical processes are both modified overall (Wu, 1979a) and modulated locally (Okuda *et al.*, 1977) by long waves. The overall modification is interesting, as discrepancies exist between physical parameters, such as wind-stress coefficients, determined in laboratories and in the field with dominant waves differing drastically in length (Wu, 1969). The local modulation is important, as it causes significant changes in the rate of momentum transfer from wind to waves (Gent and Taylor, 1976).

In the present study, experiments have been performed in a wind–wave tank with and without pre-existing long waves to evaluate more closely these effects. First of all, the wind-stress coefficient over pre-existing waves was found to be increased at low winds and reduced at high winds; while the water surface was confirmed to become smoother at all wind velocities. The wind stress acting on the windward face of long waves was found to be greater than that on the leeward face. These results are shown to be consistent with other findings.

2. Experiments and results

a. Experiment

1) FACILITY

The experiments were conducted in the Wind-Wave-Current Research Facility, which is 1 m wide, 43 m long, and 1.3 m high with a 55 cm wind tunnel above a 75 cm water depth. The tank is also equipped with a mechanical wave generator, an oscillating wedge with adjustable frequency and stroke length.

2) MEASUREMENTS

A hot-film anemometer was used for measuring simultaneously velocity components in horizontal (u) and vertical (w) directions. The anemometer was mounted on a vertical traversing mechanism, and its signals were sent to a mini-computer to obtain mean velocities, $\bar{u}$ and $\bar{w}$, as well as the averaged product of velocity fluctuations, $-\overline{u'w'}$. Waves were measured with a capacitance wave probe, supported vertically at the test section.

3) EXPERIMENTAL CONDITIONS

Two series of experiments—with and without pre-existing long waves—were conducted at a fetch of 15 m under six different wind velocities up to 14 m s^{-1}. The pre-existing long waves, produced by the mechanical generator, are 4 cm high and 100 cm long. These waves were selected with their resultant profile remaining nearly regular at all wind velocities and just reaching the point of being irregular at the highest wind velocity. The average height (H) and length (λ) of waves for cases with and wihtout pre-existing long waves are shown in Fig. 1, where U is the free-stream wind velocity. The wavelength shown in the figure was estimated from the wave frequency according to the dispersion relation.

b. Results

1) WIND PROFILE, WIND STRESS, AND ROUGHNESS LENGTH

The vertical wind profile was found to follow the logarithmic distribution (Wu, 1968):

$$\frac{\bar{u}}{u_*} = \frac{1}{\kappa} \ln\left(\frac{z}{z_0}\right), \tag{1}$$

[1] Present affiliation: Shandong College of Oceanography, Qingdao, Shandong, China.

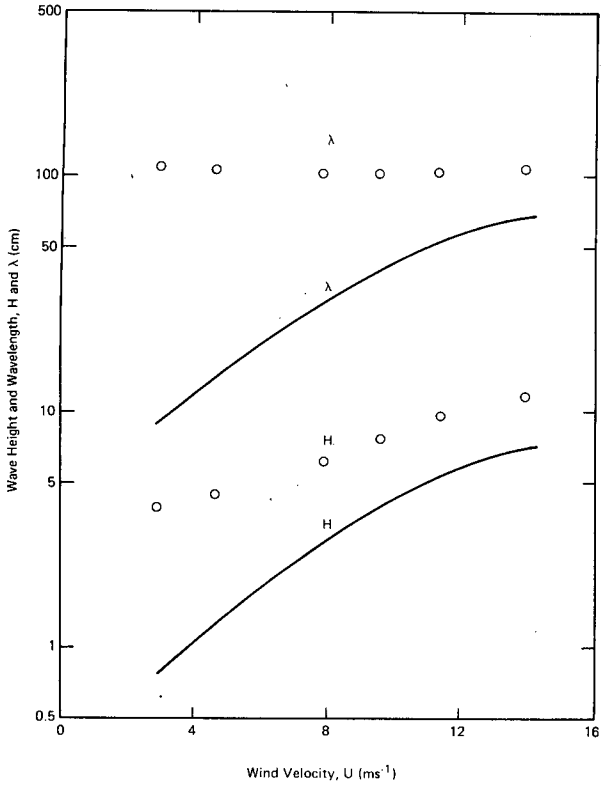

FIG. 1. Average heights (H) and lengths (λ) of waves at various wind velocities. The solid lines are for the case without pre-existing waves, and the datapoints for the case with pre-existing waves.

where $\bar{u}$ is the wind velocity measured at the elevation z above the mean water surface; u_* the friction velocity of the wind, $u_* = (\tau/\rho)^{1/2}$ (τ is the wind stress, and ρ the air density); $\kappa = 0.4$ the von Karman constant; and z_0 the roughness length. Within the constant-flux layer, we have

$$u_* = (\overline{-u'w'})^{1/2}. \quad (2)$$

In the present study, the wind-friction velocity was determined directly according to Eq. (2), use of which is necessary for the data analysis discussed in the next section. The measurements were performed at various elevations, and sample sets of data are shown in Fig. 2. A constant-flux layer as illustrated in the figure could always be identified; within this layer, the stresses were averaged. The friction velocity determined from the averaged stress was then fitted to the velocity profile to obtain the roughness length through Eq. (1). The results are presented in Fig. 3a, b.

2) WIND STRESS ON WINDWARD AND LEEWARD FACES OF LONG WAVES

For this portion of the data analysis, an analog switch was used to feed signals $u'w'$ from a designated portion of the long-wave profile to the computer. When the switch was turned on by the crest of simultaneously recorded waves and turned off by the trough, the signals from the windward face were sent to the computer. When the switch was turned on by the wave trough and off by the crest, the signals from the leeward face were sent to the computer. The friction velocities obtained through these processes are shown in Fig. 4.

3. Modification of airflow boundary layer by long waves

a. Smoothening effects of long waves

As reported earlier (Wu, 1977a), effects of pre-existing long waves on the airflow boundary layer are seen in Fig. 3 to be greater on the roughness length (presented on a logarithmic scale) than on the friction velocity (presented on a linear scale). The water surface was also found to become aerodynamically smoother at all wind velocities. A new interesting feature, however, is illustrated by the present results. At low wind velocities, the friction velocity is greater with pre-existing long waves than without; the trend is reversed at high wind velocities. These trends are not contradictory with the variation of the roughness

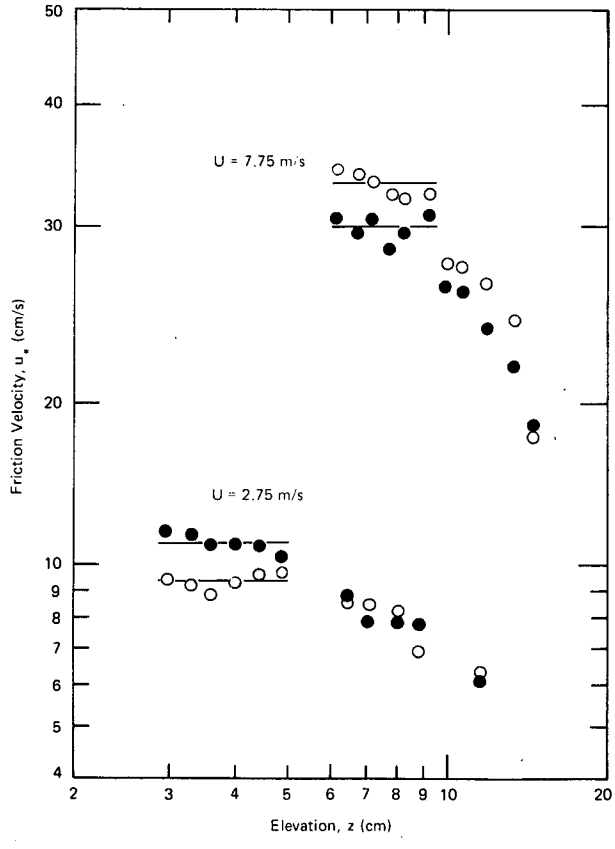

FIG. 2. Friction velocities above windward (open circles) and leeward (solid circles) faces of dominant waves.

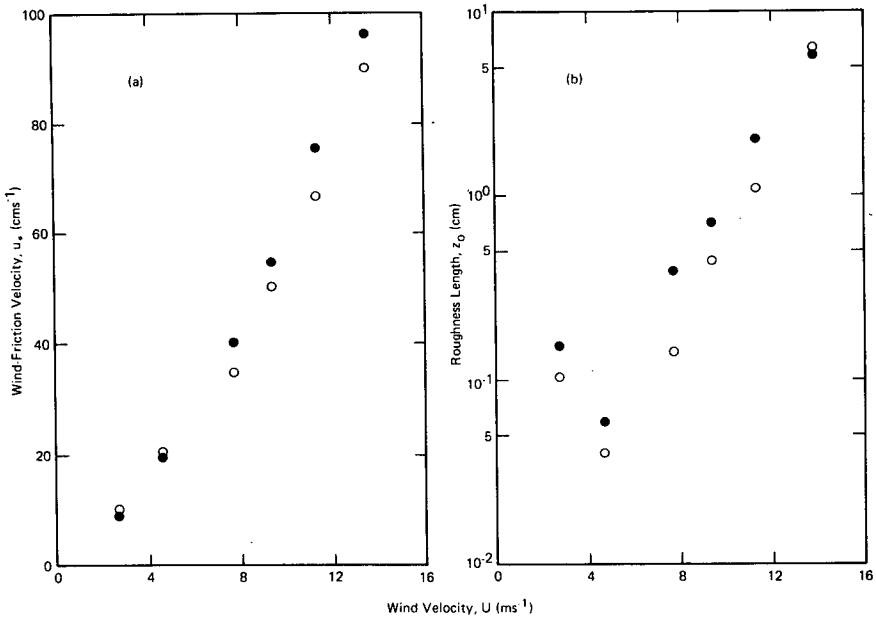

FIG. 3. Friction velocities and roughness lengths with (open circles) and without (solid circles) pre-existing waves.

length, which becomes smaller at all wind velocities with pre-existing long waves than without. They follow the concept of having two different regimes of wind–wave interaction, according to whether the interaction is governed by surface tension or gravity (Wu, 1968). As the wind-friction velocity increases, the roughness length decreases in the surface-tension regime at low wind velocities, marked by the presence of parasitic capillaries on carrier waves; the reverse is true in the gravity regime at high wind velocities, marked by breaking of carrier waves. An expression was proposed earlier (Wu, 1968) for the surface-tension regime along with the Charnock (1955) relation for the gravity regime to describe the growth of roughness length,

$$\text{Surface-tension regime:} \quad z_0 \sim \sigma/\rho_w u_*^2,$$
$$\text{Gravity regime:} \quad z_0 \sim u_*^2/g, \qquad (3)$$

where σ is the surface tension, ρ_w the density of water, and g the gravitational acceleration. In the present tank, the wind velocity dividing these two regimes is about 5 m s^{-1}. In summary, a smaller roughness length should be accompanied by a larger friction velocity at low winds, and by a smaller friction velocity at high winds. These are exactly the trends shown in Fig. 3.

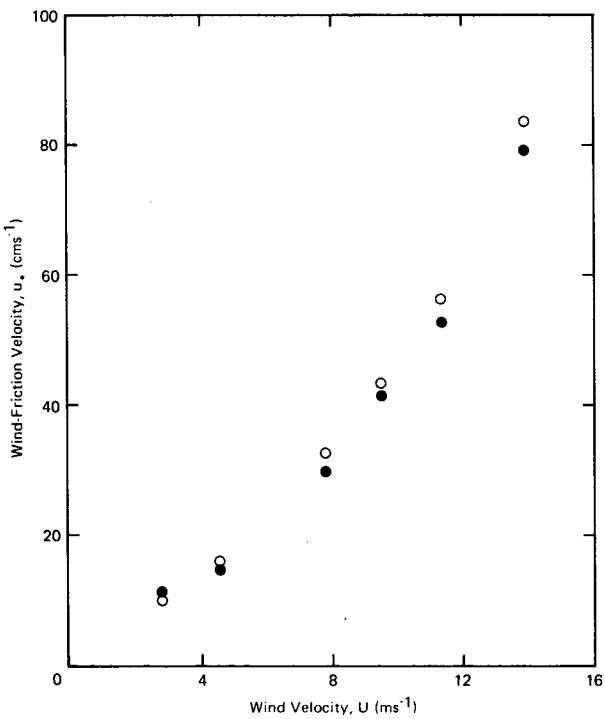

FIG. 4. Friction velocities obtained above the windward (open circles) and the leeward (solid circles) faces of dominant waves.

At low wind velocities in the surface-tension regime, capillary waves act as roughness elements; consequently, the roughness height ($30z_0$) is much smaller than the average height of dominant waves. It is well known (Schlichting, 1968) that the roughness length depends on both the height and density of roughness elements. Since capillary waves exist only locally near the crest of dominant waves, we see as discussed earlier by Wu (1977a) that a large increase in the length of dominant waves following the introduction of long waves causes a distinct reduction in the

density of roughness elements. At high wind velocities in the gravity regime, the airflow starts to separate from the crest of dominant waves. Consequently, the roughness height in the case without long waves is comparable with the height of dominant waves; see Figs. 1 and 3b. Both height and length of dominant waves are increased with the introduction of pre-existing long waves. It appears that the increase of wavelength (causing a reduction of roughness density) outweighs the increase of wave height (causing an increase of roughness height). The reduction in the density of roughness elements is due to the increase of the length of dominant wave, leaving the separation zones far apart. This is also consistent with the results shown in Fig. 3b: as the wind velocity increases with a relatively smaller increase of wavelength than wave height, the difference between roughness lengths with and without pre-existing long waves diminishes.

b. Other related studies

Measurements of wind-generated ripples were conducted earlier by Wu (1977a) with and without pre-existing long waves. The experiments were conducted in a different tank, but under similar conditions with pre-existing waves 4.5 cm high and 1 m long. The mean-square slope of the disturbed water surface was found to be much reduced with pre-existing long waves. Capillary waves, discussed earlier as the roughness elements at low wind velocities, are the main contributor to the mean-square slope. These results, therefore, provide support to the effects of pre-existing long waves on the roughness length. At high winds, the roughness elements are the dominant waves, which contribute insignificantly to the mean-square slope.

Many studies have been conducted to determine the wind-stress coefficient over the water surface; these results were compiled and reanalyzed by Wu (1969). The coefficient obtained in laboratories is generally greater than that in the field. In view of the complexity of wind-wave interaction processes, such scale effects may be caused by various mechanisms. It suffices for the present note to point out that dominant waves are very much longer in the field than in laboratories, and that smoothening effects of longer waves do not contradict the above-mentioned difference in the magnitude of wind-stress coefficients.

4. Modulation of airflow boundary layer by long wave

a. Larger shear stress on windward face

Except at the lowest wind velocity, the friction velocities above the windward face of long waves are seen in Fig. 4 to be greater than those above the leeward face. The shear stress along the wave profile was measured in a wind-wave tank by Okuda *et al.* (1977) from the distortion of hydrogen bubble lines by drift currents. Their experiments were performed under short choppy waves with a height of 0.94 cm and a length of 8.3 cm at a wind velocity of 6.2 m s^{-1}. The shear stress was found to increase continuously at the windward face toward the crest, attain the maximum value near the crest, and decrease suddenly just past the crest; the value at the leeward face was found to be essentially zero.

Undoubtedly, the local modification of the wind stress is more pronounced than that illustrated in Fig. 4, in which the results over the windward and leeward faces of long waves are respectively averaged. Nonetheless, the modification of the shear stress on the air side of the interface may never be as pronounced as that on the water side. Because water is of much greater density than air and can hardly be displaced by the wind, the airflow boundary layer bears a close similarity to the boundary layer over a solid surface. On the other hand, motions on the water side can displace air masses much easier; consequently, special characteristics of the interfacial boundary layer, such as modulation by waves; should prevail more fully.

b. Other related studies

Distribution and steepness of ripples on carrier waves were studied earlier (Wu, 1979a) with wind blowing over pre-existing long waves. The experiments were also conducted in a different facility but under similar conditions. Slope distributions of ripples located on various portions of the carrier-wave profile were obtained. At all wind velocities, the mean-square slope of ripples on the windward face is greater than that on the leeward face. The mean-square slope has been related to the wind-friction velocity (Wu, 1977b), while the time needed to establish the mean-square slope was found to be much shorter than the period of carrier waves (Wu, 1979b). In summary, the ripples represented by the mean-square slope respond instantaneously to wind stress, and the larger slope on the windward face indicates a greater wind stress there.

The present results are also consistent with the calculations of Gent and Taylor (1976) over similar wind and wave conditions, a steady airflow over an infinite train of monochromatic two-dimensional waves. The distribution of the Reynolds stress along the wave profile was found by them to have two peaks, both on the windward face. Overall, the stress is also greater on the windward than on the leeward face. The energy input from the wind to waves was also calculated by Gent and Taylor; if the roughness length is allowed to vary along the profile of long waves, the rate of transfer was found to be substantially altered.

5. Concluding remarks

The wind stress must be related to the deformed water surface; few of such correlations, however, have

been reported. Detailed studies on modification and modulation of the wind stress by long waves are worthwhile along with their effects on momentum (Longuet-Higgins, 1969; Gent and Taylor, 1976), heat, and gas transfers across the air-water interface.

Acknowledgments. We are very grateful for the sponsorship provided by the Mechanics Division, Office of Naval Research under Contract N00014-83-K-0316 and the Physical Oceanography Program, National Science Foundation under Grant OCE-8214998.

REFERENCES

Charnock, H., 1955: Wind stress on water surface. *Quart. J. Roy. Meteor. Soc.*, **81,** 639–640.

Gent, P. R., and P. A. Taylor, 1976: A numerical model of the airflow above water waves. *J. Fluid Mech.*, **77,** 105–128.

Longuet-Higgins, M. S., 1969: Action of a variable stress at the surface of water waves. *Phys. Fluids,* **12,** 737–740.

Okuda, K., S. Kawai, and Y. Toba, 1977: Measurement of skin friction distribution along the surface of wind waves. *J. Oceanogr. Soc. Japan,* **33,** 190–198.

Schlichting, H., 1968: *Boundary-Layer Theory,* McGraw-Hill, 744 pp.

Wu, J., 1968: Laboratory study of wind-wave interactions. *J. Fluid Mech.*, **34,** 91–112.

——, 1969: Froude number scaling of wind-stress coefficients. *J. Atmos. Sci.*, **26,** 408–413.

——, 1977a: Effects of long waves on wind boundary layer and on ripple slope statistics. *J. Geophys. Res.*, **82,** 1359–1362.

——, 1977b: Directional slope and curvature distributions of wind waves. *J. Fluid Mech.*, **79,** 463–480.

——, 1979a: Distribution and steepness of ripples on carrier waves. *J. Phys. Oceanogr.*, **9,** 1014–1021.

——, 1979b: Temporal rates of growth and decay of microscopic and macroscopic surface structures in a wind-wave tank. *J. Phys. Oceanogr.*, **9,** 802–814.